A Multilevel Voltage Source Inverter Filter for Power Grid Analysis and Simulation

Dr. Mahendra Kumar

[1]Guru Kashi Univerity, Talwandi Sabo

ABSTRACT

Incorporating APF technology into the aviation power system to increase the system's quality and dependability becomes a more appealing option. In order to meet with the standard recommendations, shunt active power filters are a potential alternative for power quality enhancement. By employing typical methods to adjust for the harmonics created by the nonlinear load, it is difficult to bring the system's power-quality characteristics into compliance with harmonic standards. For the aeronautical APF, a three-stage H-bridge cascaded inverter was chosen (AAPF). To boost APF's performance, the control levels are increased. The higher control level can improve the power quality and dependability of the aviation power system. The planned AAPF's global framework and operation principles are outlined in detail. The suggested AAPF uses a source current direct control method and a cascaded inverter design. The conventional system's power quality attributes aren't up to par. With traditional systems, the performance characteristics of EPS are not preferable.

Keywords— Multilevel inverters inverter, aerodynamic active and reactive filter (APF) (AAPF)

I.INTRODUCTION

Recent research on civil aviation systems has shifted to a greater use of electric power over other traditional sources like as mechanical, hydraulic, and pneumatic power. More Electric Aircraft is the name given to this technical trend. Recent advancements in the fields of power electronics, electric devices, control electronics, and microprocessors have allowed aircraft electrical systems to function better than ever. The usage of extra electric power has significant benefits for the whole system's operation. These benefits are outlined below. Advantages of expanding electric power utilisation in aircraft systems include:

- optimization of the performance
- optimization of the life cycle cost
- reduction of weight and size of the equipment
- increased reliability

There are significant adjustments made. Because of the increased use of electric power on board, significant changes have been made to the aircraft electrical system. These modifications are listed below. Consequences of increased use of electric power on the electrical system of aircraft:

- more electrical loads

- more complex topology of the electrical network
- more generation demand
- more power electronic equipment
- more stability issues
- more power quality issues

These aspects have to be taken into account when designing the devices in the system.

A high-performance aeroplane APF is proposed in this research. The proposed aeronautical APF (AAPF), unlike typical open-loop control strategies, operates in a closed-loop mode. The unique AAPF is used to achieve good EPS power quality. A feed forward path of the load current is also included to increase the dynamic performance of the load response. The operating concept of the feed forward compensation path is discovered based on the modelling and analysis of the close-loop system. Meanwhile, the cascaded-inverter-based AAPF's control approach is proposed. The overall voltage control and voltage-balance control operation principles are presented. The simulation results are presented for various fundamental frequencies and load circumstances. An aircraft APF system with a 7.2-kVA load power is created and tested in the laboratory to verify the aforementioned analysis and compensation performance of the proposed AAPF.

II. CLOSE-LOOP CONTROL STRATEGY AND ITS FEED FORWARD COMPENSATION

2.1. Close-Loop Control Strategy

The current reference in classic APF control is usually the harmonic and reactive components of the load currents. The technique, which is based on feed forward open loop control, is, however, susceptible to parameter mismatches and relies on the ability to precisely estimate the voltage-source inverter current reference and its control performance [5]–[7]. The source current is the detection and control target in close-loop control. The fundamental frequency of the aeroplane EPS is substantially greater than that of a 50-Hz power system. Measurement mistakes, analog-to-digital conversion time, digital latency, and other non-ideal conditions will all exacerbate the open-loop compensating effect. As previously stated, feedback control provides the following advantages: It may lower the sensitivity of the transfer function from the reference input to the output to disturbances, and it may make the transfer function from the reference input to the output insensitive to changes in the gains in the forward path. As a result, close-loop control is more suitable for aeronautical applications than open-loop control.
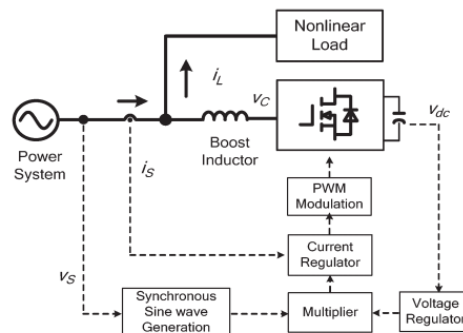
Fig. 1. Control diagram of source current direct control.

2.2. Source Current Direct Control

The principal control strategy of the proposed AAPF is close-loop control, also known as source current direct control. In [16], Wu and Jou suggest source current direct control. The close loop control scheme's basic system diagram is shown in Figure 1. The following is how this control scheme works: The voltage regulator receives the dc-link voltage, and the regulator's output, as well as a synchronous sine wave detected from the phase voltage, is sent to the multiplier. The multiplier's output is delivered to the current regulator, which serves as the source current reference. To generate the pulse width modulation waveforms, the current regulator's output will be transmitted to the modulator. This compensation strategy's comparable control model is shown in Figure 2. The source current reference of the source current direct control is derived from the variation of the dc-link voltage, as shown in Fig. 2. Gv(s) denotes the voltage controller's transfer function, and Kf is the dc-link voltage detection coefficient.
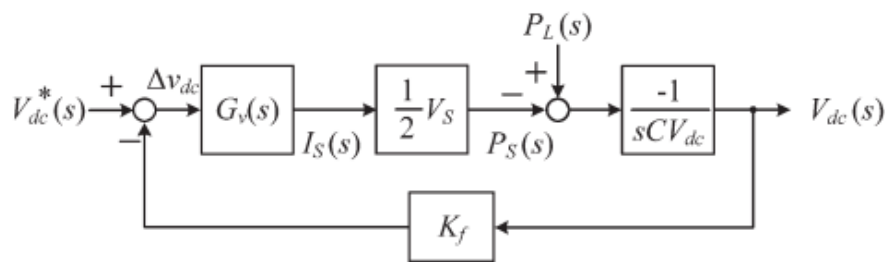
Fig. 2. Model for active power analysis.

2.3. Load Current Feed forward Compensation

Load power PL(s) acts as a disturbance factor in the APF system, as shown in Fig. 2. PL(s) and Vdc (s) have the same transfer function.

$$\Phi_{en}(s) = \frac{\Delta V_{dc}(s)}{P_L(s)} = \frac{\frac{1}{sCV_{dc}}K_f}{1 + G_v(s) \cdot \frac{1}{2}V_s \cdot \frac{1}{sCV_{dc}} \cdot K_f} \tag{1}$$

The transfer function between IL(s) and I∗S(s)is

$$H_{iL}(s) = \frac{I_S^*(s)}{I_L(s)} = \frac{\Delta V_{dc}(s)G_v(s)}{P_L(s)/\left(\frac{1}{2}V_s\right)} = \Phi_{en}(s) \cdot \frac{G_v(s)}{\frac{1}{2}V_s}$$
$$= \frac{G_v(s) \cdot \frac{1}{2}V_s \frac{1}{CV_{dc}}K_f}{s + G_v(s) \cdot \frac{1}{2}V_s \frac{1}{CV_{dc}}K_f} = \frac{A \cdot G_v(s)}{s + A \cdot G_v(s)} \tag{2}$$

Where A=Vs Kf/ (2CVdc).

HiL(s) |f=50 depicts the present reference's dynamic speed in response to a change in load power at fundamental frequency. In general, a high dynamic response is required for an APF system, which means a higher HiL(s)|f=50 value is preferred. However, numerous additional factors, such as the voltage controller, line voltage, dc-link voltage, dc-link capacitor, and voltage detection coefficient, affect HiL(s). The bode diagram of HiL(s) under various voltage controllers and coefficient A is

shown in Fig. 3. When the dc-link voltage is 800 V, the dc-link voltage detection coefficient Kf is 0.005, and the dc-link capacitor is 6800F, coefficient A translates to 0.14 for an APF system used in a 220-V/50-Hz application. With such a low value of A, designing a voltage controller to obtain a high value for HiL(s) |f=50 at 50 Hz is difficult. When the dc-link voltage is 600 V, the dc-link voltage detection coefficient Kf is 0.005, and the dc-link capacitor is 3300F, the phase voltage is only 115 V, causing A to be 0.2. It signifies that both programmes have a poor dynamic response. A feed forward compensation path is introduced to lessen the disturbance effect of the load current in order to increase the dynamic speed reacting to load changes, as shown in Fig. 3. F(s) is the low-pass filter's (LPF) transfer function, which extracts the fundamental elements of the power flows.
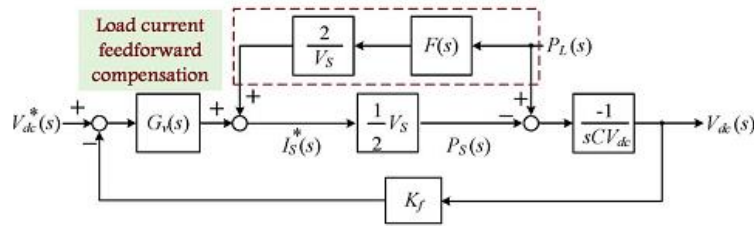
Fig.3.Disturbance compensation-based lose-loop control.

$$F(s) = \frac{\omega_0^2}{s^2 + \sqrt{2}\omega_0 s + \omega_0^2}$$

(3)

The cutoff angular frequency of the LPF is 0=2fc in this case. The transfer function between IL(s)and IS(s)becomes once the fundamental of the load current is feed forward. The magnitude of HiL(s)|f=50 is enhanced once the load current is fed forward. The selection off, on the other hand, is critical to HiL (s); fc should typically be greater than the fundamental frequency.

III. CONTROL METHOD OF THE CASCADED-INVERTER-BASEDAAPF

3.1. Discussion and Demonstration on the Power Stage of AAPF

A shunt APF is a controlled harmonic current source that injects current that is inversely proportional to the load harmonic. The 11th and 13th harmonic frequencies in the 400-Hz aeroplane EPS are as high as 4.4 and 5.2 kHz. One of the most challenging aspects of constructing AAPF is determining how to accurately draw a high-frequency harmonic current.
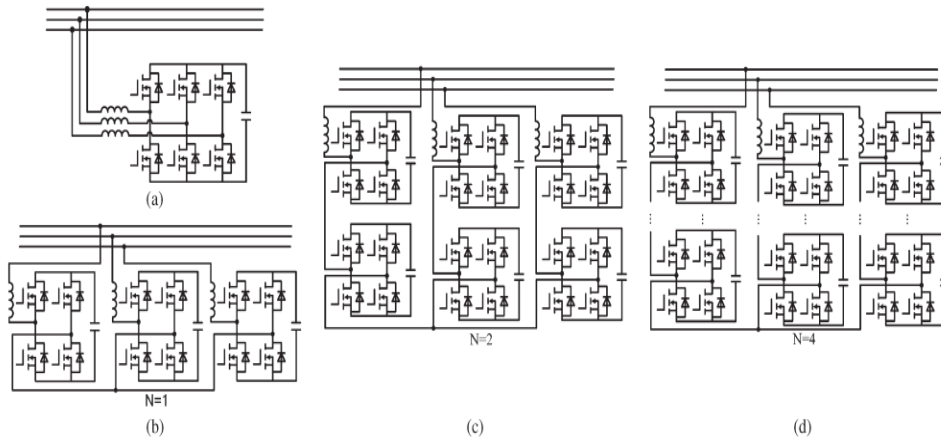
Figure 4: AAPF's four probable options. (a) APF based on three-leg inverters. b) APF based on H-bridges. (c) APF with two H-bridges cascaded. (d) APF with four H-bridges in a cascade.

The three leg-inverter-based APF, the H-bridge-based APF, the two H-bridge cascaded APF, and the four H-bridge cascaded APF are all possible AAPF options, as shown in Figure 4. A comparison of these options is presented below. In the first solution, the AAPF switching frequencies are set to 60, 120, and 240 kHz, and the dc-link voltage is adjusted to 400 V to provide good current tracking performance in a 400-Hz system. In the second solution, the switching frequencies of AAPF are chosen as 30, 60, and 120 kHz, and the dc-link voltage is 300 V, taking into account the "double equivalent switching frequency impact" of the carrier phase shift (CPS) PWM modulation. Meanwhile, the same similar switching frequency translates to nearly same current tracking performance and AAPF bandwidth. Table I shows power switches from International Rectifier (IR) Corporations, all of which have a current rating of around 24 A. The switching losses and conductive losses of the power MOSFET could be assessed using the following switching loss estimation method:

$$P_{SW} = \frac{1}{2} I_D V_D (t_{OFF} + t_{ON}) f_{sw} + \frac{1}{2} C_{OSS} V_D^2 f_{sw}$$

(4)

$$P_{con} = \bar{I}_{RMS}^2 R_{ds(on)} D + V_{DF} I_D (1 - D)$$

(5)

PSW and P concor are the switching and conductive losses, respectively, while ID, VD, and fsw are the drain current, bus voltage, and switching frequency, while tON and tOOF Fare are the power MOSFET turn-on and turn-off timings. The output capacitance and on-resistance of the power MOSFET are COSSRds (on), and VDF is the forward voltage drop of the power MOSFET's reverse parallel diode.
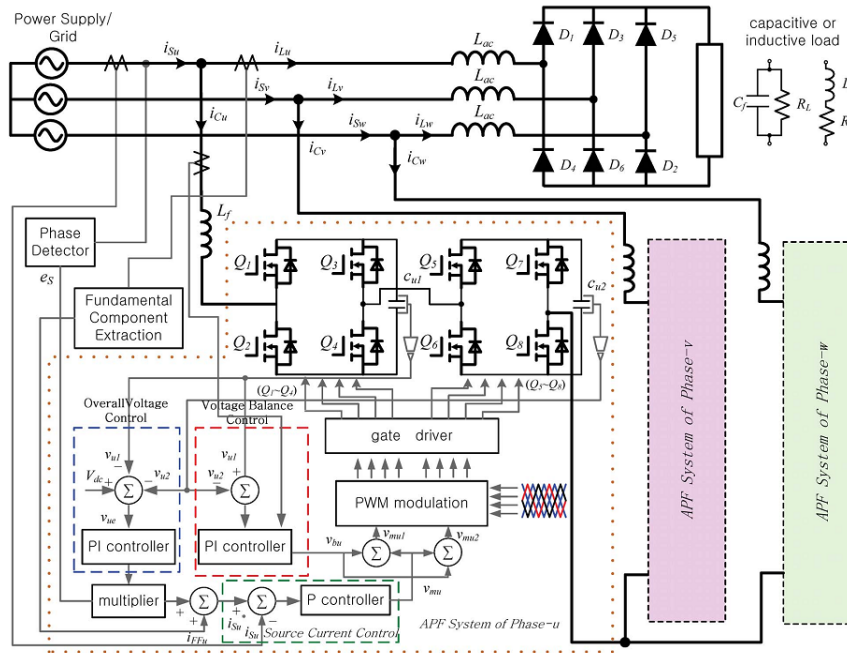
Fig. 5. System diagram of the proposed AAPF.

The two H-bridge cascaded APF is chosen as the power stage configuration of the AAPF in this work because of the acceptable modest power loss and reliability (as shown in Fig.5). The switching frequency is set to 30 kHz, resulting in a five-level line-to-neutral PWM waveform with the lowest harmonic sideband centred at 120 kHz (= 30 kHz2) for each cluster. The capacitors' voltage balance must be maintained for the H-bridge-based AAPF to operate safely. The floating dc capacitors' voltage-balance management can be split into the following categories:

1) Clustered overall control.

2) Balancing control.

3.2. Clustered Overall Control

The control target in the cluster overall voltage control loop is the average of the capacitor voltages for each cluster (for example, vu1 and vu2 for phase-u). This cluster overall control creates the u-phase clustered overall voltage signal vou from the dc capacitor voltage reference vdc, the dc capacitor voltages of the u-phase cluster vu1,vu2, and the synchronous sine wave eSu (as shown in Fig. 6). NH-bridge cascaded inverter topologies might potentially benefit from this voltage control strategy. N stands for the number of cascaded converter units. When one or more cascaded units fail, the ultimate compensation performance does not worsen, which is an obvious advantage of this control system.
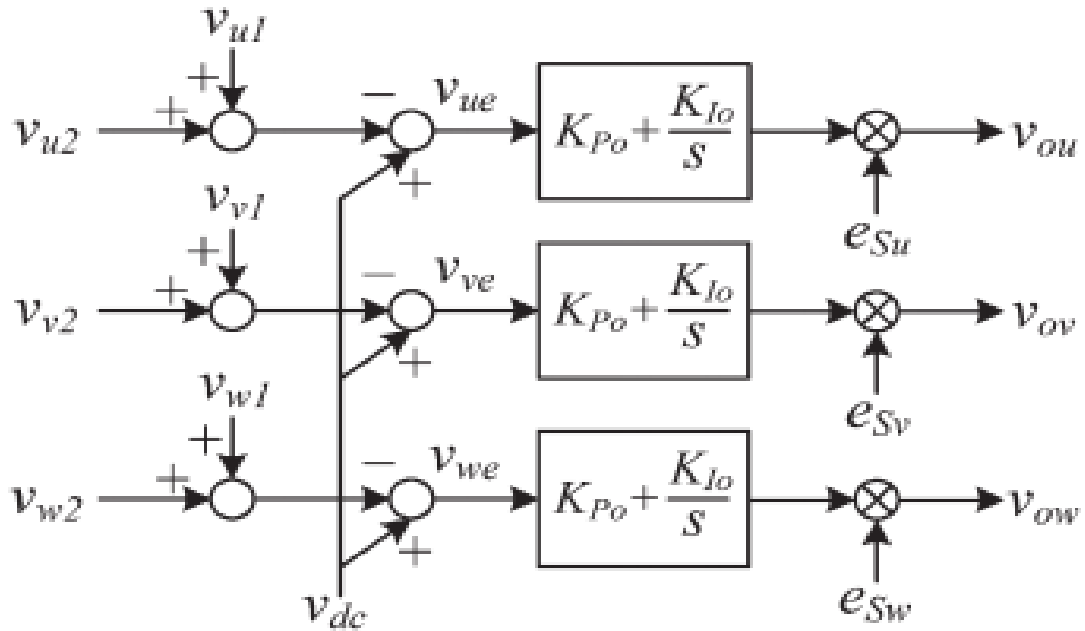
Fig. 6. Control diagram of the cluster overall control.

The remaining cascaded units would share the defective unit's dc-link voltage. This voltage management strategy can improve the AAPF system's fault tolerance and dependability.

Fig. 7. Operation principle of voltage-balance control. (a) Control diagram. (b) Regulation procedure.

3.3. Balancing Control

The balancing control produces a balance control signal vbn (n=u, v, w) to make the voltage of the capacitors in each cluster balanced, as shown in Fig. 7(a). From the origin modulation wave vm and the dc capacitor voltages of each cluster vn1, vn2, the individual balancing control generates two modulation wavesvmn1andvmn2. Vmn1 modulates PWM signals for Q1, Q2, and Q3, Q4, whereas Vmn2 modulates PWM signals for Q5, Q6, and Q7, Q8 in the CPS PWM modulation. The charging or discharging of each capacitor in the dc link is determined by the current direction and switch combination. The voltage signal vbu should be added or removed from the amplitude modulation depending on the current direction and required charging or discharging operation. When the duty cycles of Q1andQ4decrease, the input power of the top cascaded unit decreases, resulting in a reduction in the dc-link voltage vu1. Similarly, the lower cascaded unitvu2's dc-link voltage will be increased. As a result, the voltage balance is achieved. Take the phase-u cluster as an example to demonstrate the voltage-balance control regulation process [as illustrated in Fig. 7(b)]. The modulation wave of bridge 1 (which consists of Q1 and Q2) is vmu in the steady state, and the conduct times of Q1 and Q2 are tu1 and tu2, correspondingly. When the circumstance vu1> vu2 occurs, the regulator generates a positive balance control voltage signal vbu. The final modulation wave for Q1 and Q2 is the sum of vmu and vbu, which becomes vmu1 after regulation, as shown in Fig. 7(a). As a result, the conduction times of Q1 and Q2 become t'u1 and t'u2, respectively. As shown in Fig. 7(b), we discovered that t'u1 tu1 and t'u2>tu2, implying that Q1's duty cycle reduced while Q2's duty cycle rose.
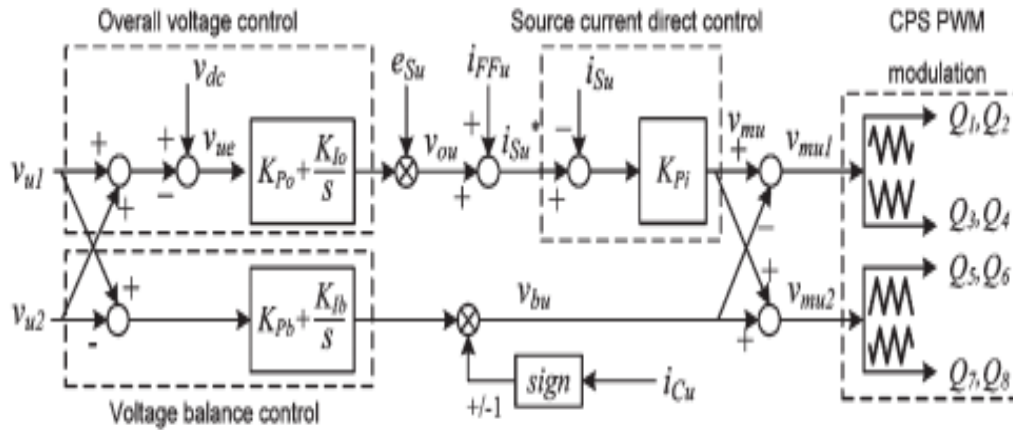
Fig. 8.Control diagram for phase-u of the proposed AAPF.

In the meantime, Q3's duty cycle grew while Q4's duty cycle fell. Figure 8 depicts the entire phase-u control diagram for the proposed AAPF, which includes overall voltage control, voltage-balance control, load current feed forward compensation, and source current direct control.

IV. MATLAB/SIMULINK RESULTS
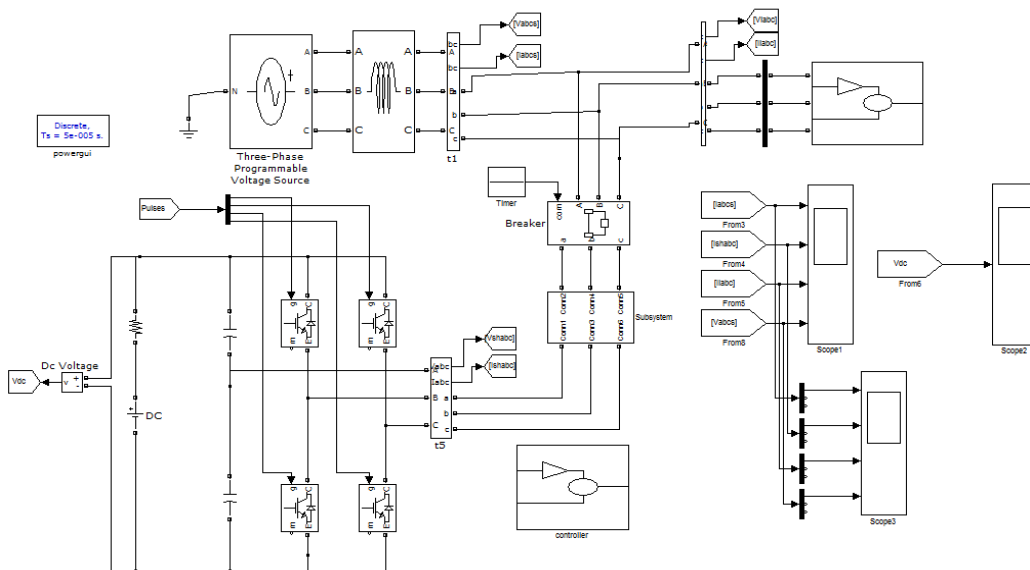
Fig. 9. Matlab/Simulink model of inductive load.
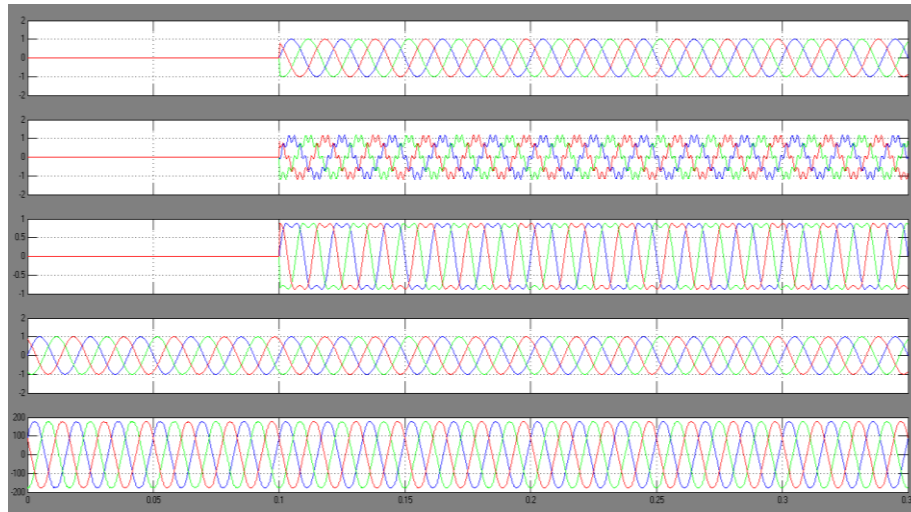
Fig. 10. Inductive load of sinusoidal phase voltage and distorted phase voltage.
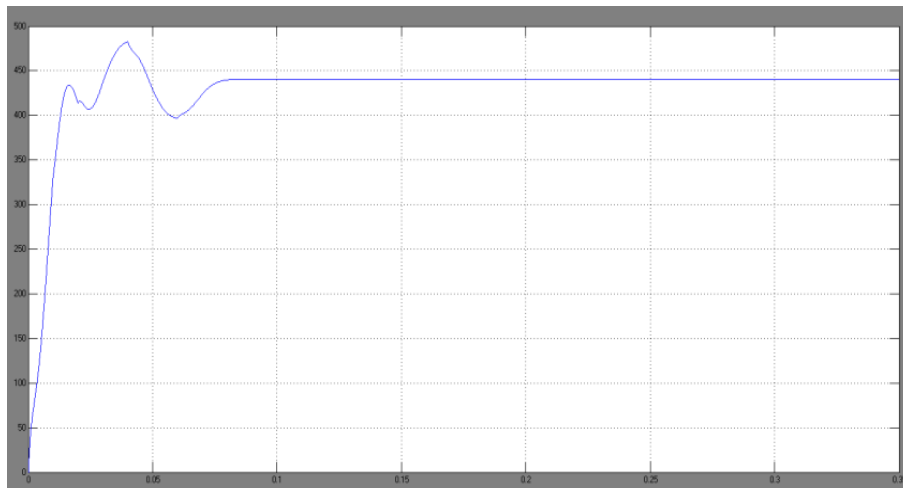
Fig. 11. DC capacitor voltage waveforms under loading.
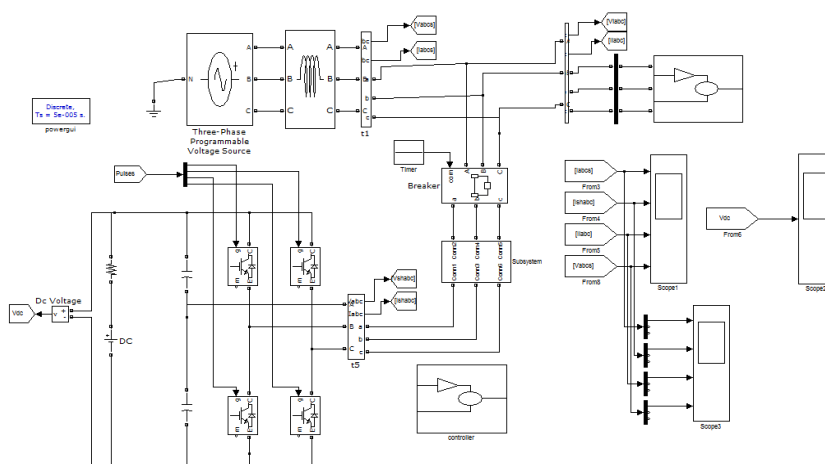
Fig. 12. Matlab/Simulink model of capacitive load
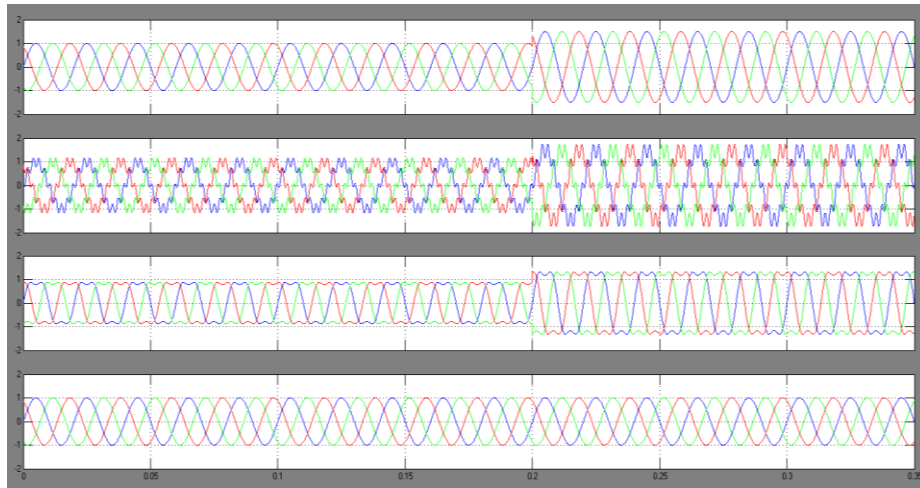
Fig. 13. Waveforms under loading.
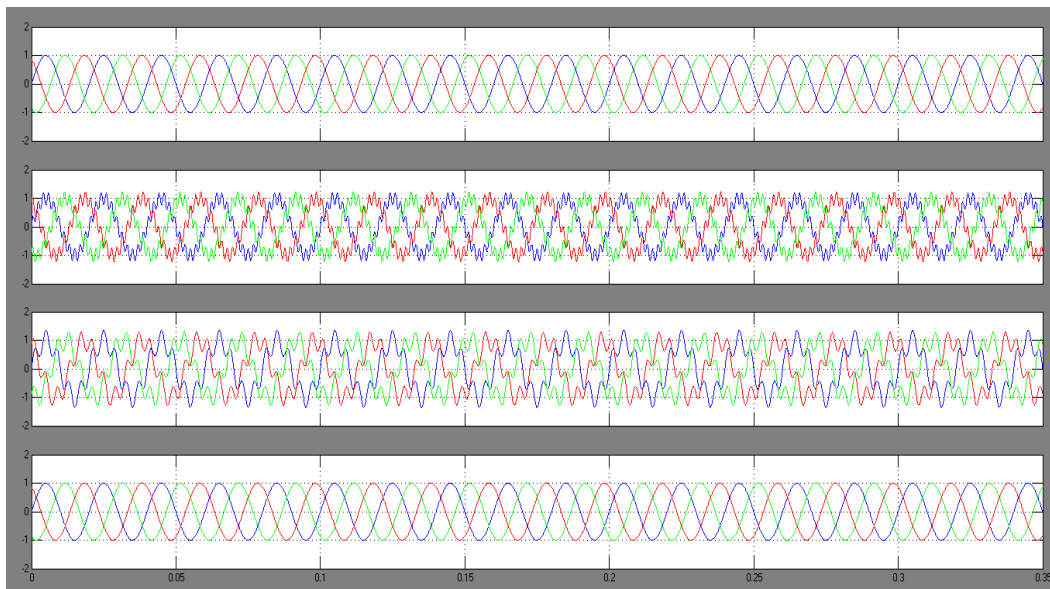
Fig. 14. Simulation waveforms of AAPF under variable-frequency EPS.

V.CONCLUSION

APF technology is a good way to overcome the power quality problems that current aircraft EPS have. The source current direct control-based AAPF has a load current feed forward compensation mechanism proposed in this research. The cascaded-inverter based active filter system's appropriate system control approach is shown. The seven-level control approach for the cascaded-inverter based active filter system is displayed. The simulation results reveal that the suggested control system has appropriate compensating behaviour for many types of load conditions and has outstanding dynamic response.

REFERENCES

1. J. A. Rosero, J. A. Ortega, E. Aldabas, and L. Romeral, "Moving towards a more electric aircraft,"IEEE Aerosp. Electron. Syst. Mag., vol. 22, no. 3, pp. 3–9, Mar. 2007.
2. A. Hamadi, S. Rahmani, and K. Al-Haddad, "A hybrid passive filter configuration for VAR control and harmonic compensation, "IEEE Trans. Ind. Electron., vol. 57, no. 7, pp. 2419–2434, Jul. 2010.
3. A. Varschavsky, J. Dixon, M. Rotella, and L. Moran, "Cascaded nine-level inverter for hybrid-series active power filter, using industrial controller," IEEE Trans. Ind. Electron., vol. 57, no. 8, pp. 2761–2767, Aug. 2010.
4. A. Luo, X. Xu, L. Fang, H. Fang, J. Wu, and C. Wu, "Feedback– feed forward PI-type iterative learning control strategy for hybrid active power filter with injection circuit, "IEEE Trans. Ind. Electron., vol. 57, no. 11, pp. 3767–3779, Nov. 2010.
5. S. Rahmani, N. Mendalek, and K. Al-Haddad, "Experimental design of a nonlinear control technique for three phase shunt active power filter," IEEE Trans. Ind. Electron., vol. 57, no. 10, pp. 3364–3375, Oct. 2010.
6. B. Singh and J. Solanki, "An implementation of an adaptive control algorithm for a three-phase shunt active filter, "IEEE Trans. Ind. Electron., vol. 56, no. 8, pp. 2811–2820, Aug. 2009.
7. A. Bhattacharya and C. Chakra borty, "A shunt active power filter with enhanced performance using ANN-based predictive and adaptive controllers," IEEE Trans. Ind. Electron., vol. 58, no. 2, pp. 421–428, Feb. 2011.
8. D. Ganthony and C. M. Bingham, "Integrated series active filter for aerospace flight control surface actuation," in Proc. EPE, 2007, pp. 1–9.
9. E. Lavopa, E. Summer, P. Zanchetta, C. Ladisa, and F. Cupertimo, "Real time estimation of fundamental frequency and harmonics for active power filters applications in aircraft electrical systems," in Proc. EPE, 2007, pp. 4220–4229.
10. E. Lavopa, M. Summer, P. Zanchetta, C. Ladisa, and F. Cupertimo, "Real-time estimation of fundamental frequency and harmonics for active power filters applications in aircraft electrical systems, "IEEE Trans. Ind. Electron., vol. 56, no. 8, pp. 2875–2884, Aug. 2009.
11. M. Odavic, P. Zanchetta, and M. Summer, "A low switching frequency high bandwidth current control for active shunt power filter in aircrafts power networks," in Proc. IEEE IECON, 2007, pp. 1863–1868.